Evolution and dynamics of the denitrification in the Arabian Sea on millennial to million-year timescale

Shubham Tripathi*, Padmasini Behera and Manish Tiwari

National Centre for Polar and Ocean Research, Ministry of Earth Sciences, Vasco-da-Gama, Goa 403 804, India

Denitrification in the Arabian Sea is a vital process that provides feedback to global warming by releasing nitrous oxide to the atmosphere. Therefore, it is important to understand the evolution and dynamics of denitrification on different timescales. We present here the denitrification variability spanning the past ~600 thousand years (kyr). It is based on ~300 new measurements from IODP 355 Expedition. We compared the existing records of denitrification to understand the factors influencing the denitrification on various timescales. On glacial–interglacial timescale, we find stronger denitrification during interglacial and weaker denitrification during glacial periods. During the Holocene, we observe declining denitrification in the Western Arabian Sea in response to the reduced monsoon-induced productivity but find increasing denitrification in the Northeastern Arabian Sea due to reduced ventilation.

Keywords: Arabian Sea, denitrification, geochemistry, monsoon, oceanic circulation, palaeoceanography, stable isotopes.

Introduction

THE Arabian Sea has one of the strongest perennial oxygen minimum zones (OMZ) of the world oceans where oxygen concentration drops to less than 20 μM (ref. 1). This perennial OMZ is formed at a water depth of around 150 m to 1200 m due to high oxygen consumption for the respiration of a large amount of organic matter produced in the upwelling dominated Western Arabian Sea[2,3]. The organic matter produced in the Western Arabian Sea during the southwest monsoon is advected towards the Eastern Arabian Sea and the Central Arabian Sea. Thus, a continuous organic matter supply stabilizes the perennial OMZ in the Eastern Arabian Sea. The development of this OMZ is further supported by poor ventilation by subsurface currents and a strong stratification due to tropical thermocline because of relatively high SST that inhibits the mixing with the oxygen-rich surface water[2,3]. As the Arabian Sea is closed by landmass on its northern border, there is an absence of any major oxygen-rich deep to intermediate water inflow from that side as well[4]. Once the oxygen level falls below 1 μM (ref. 5), nitrate (NO_3^-) is used as an oxidizing agent (electron acceptor) for the bacterial respiration (oxidation) of organic matter resulting in denitrification. During denitrification, the nitrate (oxidation state, OS: +5) is reduced to nitrite (NO_2^-; OS: +3), nitric oxide (NO; OS: +2), nitrous oxide (N_2O; OS: +1) and finally to gaseous nitrogen (N_2; OS: 0). Thus, denitrification releases gaseous products like N_2O and N_2 that, to a large extent, are lost to the atmosphere so there is a net loss of fixed nitrogen from the ocean during denitrification[6,7].

Post-industrialization, anthropogenic climate change is projected to enhance sub-oxic conditions in large regions of the world ocean[8,9] that would result in the expansion of the OMZs. It would increase the production of nitrous oxide, which is a major greenhouse gas. Additionally, denitrification reduces the oceanic nitrate inventory – a limiting nutrient – that would result in a lower drawdown of CO_2 due to reduced productivity and thus provides positive feedback to the global warming[10,11]. Considering the importance of denitrification to climate change, it is important to understand the denitrification variability in the Arabian Sea and its controlling mechanisms on various time scales. The residence time of fixed nitrogen in the ocean is ~3000 years thus the marine nitrogen inventory is altered in several thousand years[12]. Here, we present a new record of denitrification spanning a period from 600 thousand years before present (kyr BP) to 50 kyr BP from the eastern Arabian Sea using sediment cores recovered during the IODP 355 expedition. This is a unique record spanning such a long period at millennial-scale resolution. We also examine the existing records of denitrification to discuss the evolution and denitrification mechanism in the Arabian Sea on millennial to million-year time scales.

Nitrogen isotopes of nitrate as a proxy of denitrification intensity

Nitrogen has two stable isotopes, namely ^{14}N and ^{15}N with abundances of 99.64% and 0.36% respectively. The nitrogen isotopes mostly undergo 'kinetic fractionation'

*For correspondence. (e-mail: shubham@ncpor.res.in)

in the marine nitrogen cycle as most of the reactions are biologically mediated. The isotope fractionation (ε) in this case can, therefore, be expressed as the deviation of the ratio of the 'rate coefficients', viz. ^{14}K and ^{15}K of the reaction for the reactants containing lighter (^{14}N) and heavier (^{15}N) isotopes respectively, from unity. As it is a small number so it is further multiplied by 1000 for ease of comprehension and is expressed in per mil. So, ε(‰) = $(^{14}K/^{15}K - 1) \times 10^3$. The isotope fractionation during the process 'nitrogen fixation' (the reduction of N_2 to NH_4^+, and oxidation to NO_2^- and NO_3^- and their subsequent assimilation into the organic matter) is less than 2‰ resulting in a slight decrease of the $\delta^{15}N$ values of the particulate nitrogen[13]. Nitrate uptake/utilization also results in small fractionation (ε = ~5‰) and a slight increase in $\delta^{15}N$ values; more the relative nutrient (nitrate) utilization, more will be the $\delta^{15}N$ value[10,14]. The isotope fractionation for benthic denitrification (occurring due to anoxia within the sediments) is negligible (ε = ~0‰) because nitrate is almost 100% consumed in the sediment pore environment. The largest isotopic fractionation takes place during the denitrification process in the water column at the depth of ~200 to 300 m – the pelagic denitrification[15]. The isotope fractionation value is around 25‰ resulting in very high $\delta^{15}N_{NO_3^-}$ that can go up to 15‰ and above[16]. In the Arabian Sea, previous studies have shown that nitrate utilization does not play an important role in affecting $\delta^{15}N_{NO_3^-}$ (ref. 17). Nitrogen fixation can be an important process in oligotrophic, stratified waters and in waters overlying denitrifying zones resulting in lower surface $\delta^{15}N_{NO_3^-}$ (ref. 18). However, the waters overlying the Arabian Sea denitrification zone have high $\delta^{15}N$ values reflecting the fact that denitrification in the Arabian Sea is the dominant process governing the $\delta^{15}N_{NO_3^-}$ values. This nitrate enriched in heavier isotope is upwelled to the euphotic zone and is consumed by the organic productivity, a fraction of which finally gets preserved in the sediments resulting in relatively higher $\delta^{15}N$ values of the sedimentary organic matter (SOM) underlying the denitrification zones[10,19,20].

Oceanic circulation at intermediate depth

There are three distinct water masses present at the intermediate depth (200–1000 m) of the Arabian Sea originating from Northwestern (Red Sea Water (RSW), Persian Gulf Water (PGW)) and Southern (Indian Central Water (ICW)) Indian Ocean[21–23]. Other water masses like aged Antarctic Intermediate Water (AAIW) and Banda Sea Water (BSW) also enter the Arabian Sea through southwestern boundary and move towards the northeastern Arabian Sea via Somali Current[23,24]. Presently, the AAIW spreads up to 5°N in the Indian Ocean and from there it feeds to ICW[23]. The inflow of AAIW to the Arabian Sea varies with the mean sea level and the fronts created by other water masses. During glacial periods, the decrease in sea level reduces the inflow of high saline water (RSW and PGW) to the Arabian Sea[25,26]. The absence of this very saline water from marginal seas with strongly reduced BSW (low salinity front created along the equator) favours the northward circulation of the oxygen-rich AAIW (shown in Figure 1 *a* by thick blue arrows). But during interglacial periods, the increase in sea level favours the expansion of a strong frontal system along the equator and the inflow of highly saline marginal water to the Arabian Sea. This causes the reduced inflow of the southern oxygen-rich AAIW into the Arabian Sea (shown by the thin blue arrow in Figure 1 *b*)[27].

Materials and methodology

Site setting and core description

The site U1457 (17°9.95′N, 67°55.80′E, water depth 3534 m) was drilled in the Laxmi Basin located in the

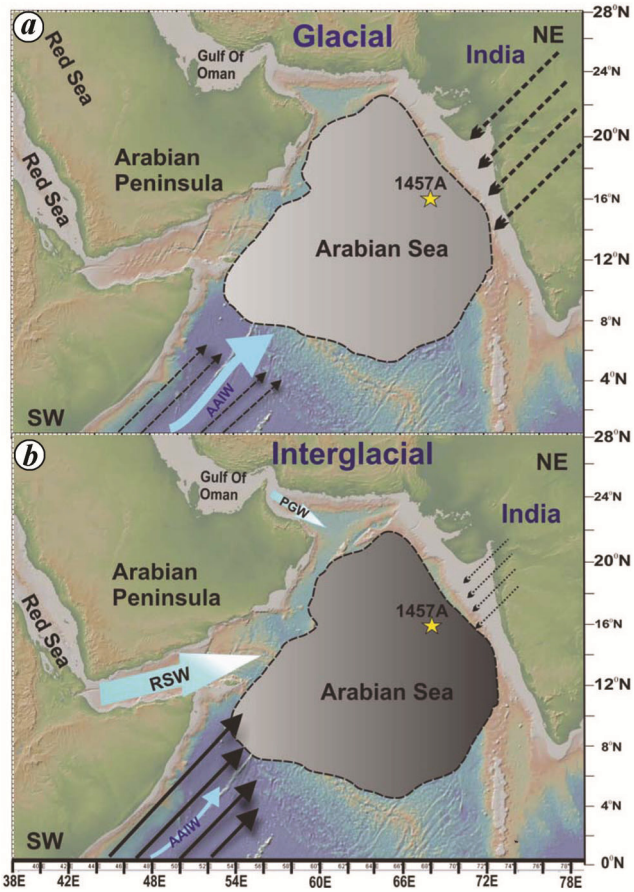

Figure 1. Location map and schematic diagram of the Arabian Sea. (***a***) and (***b***) show southwest and northeast monsoon wind (black arrows) and intermediate water flow (blue arrows) during glacial and interglacial periods respectively. Thicker arrows reflect stronger winds/circulation. The present study site (U1457) is shown by yellow star. Denitrification gradient during the glacial and interglacial period is shown in grey colour (darker colour indicates stronger denitrification).

eastern part of the Indus Fan during IODP Expedition 355 (Figure 1). IODP site U1457 is located ~490 km west of the Indian coast and ~760 km south from the modern mouth of Indus River. In this study, we used the upper ~43 mbsf of sediment core (U1457A) corresponding to the last ~40 kyr to ~600 kyr (ref. 28). The lithology of the studied sections consists of light brown to light green nannofossil ooze including foraminifer-rich nannofossil ooze and nannofossil-rich clay, interbedded with silty clay and silty sand[28].

Nitrogen isotope ratio and concentration analysis

Bulk sediment samples were powdered, and 200 mg was used for nitrogen concentration and nitrogen isotope ratio analysis of the sedimentary organic matter. Samples of ~130 mg weighed out into 8–6 mm tinfoil cups and analysed using Elemental Analyser coupled with 'isoprime dual inlet isotope ratio mass spectrometer' at the Marine Stable Isotope Laboratory (MASTIL) of National Centre of Polar and Ocean Research (NCPOR), Goa, India. The isotopic values are expressed in terms of delta (δ) notation, which is the relative difference of isotopic ratios in the sample from an international standard. Thus: $\delta^{15}N = \{(^{15}N/^{14}N)_{sample}/(\delta^{15}N/^{14}N)_{standard}\} - 1$; where $(\delta^{15}N/^{14}N)_{sample}$ and $(\delta^{15}N/^{14}N)_{standard}$ are the ratios of the abundances of the less abundant (heavier, i.e. ^{15}N) to more abundant (lighter, i.e. ^{14}N) isotope in the sample and standard respectively. The $\delta^{15}N$ value is multiplied by 10^3 for the ease of readability and comprehension and is therefore expressed in per mil (‰). The reproducibility of $\delta^{15}N$ measurement is ± 0.12‰ (1σ standard deviation) based on the repeat measurement of the IAEA-N1 ammonium sulphate standard. The $\delta^{15}N$ values are quoted with respect to air–N_2. The reproducibility of total nitrogen measurement is ±0.70% (1σ) based on the repeat measurement of the sulphanilamide standard.

Age–depth model

The age model of IODP site U1457 is based on linear sedimentation rate using the age–depth model generated on-board *JOIDES Resolution*. The on-board age-depth model was based on the first and the last appearance of planktic foraminifera, nannofossils and palaeomagnetic reversals[28]. The age model, the upper 43 mbsf of IODP site U1457 provides a continuous record of the last ~600 kyr, with an average linear sedimentation rate of ~7.0 cm/kyr.

Results and discussion

Denitrification on a million-year time scale

Although there is a paucity of data to describe denitrification through geological time scale, we revisited some records from different ocean basins of the world which extend past into deep geological time. Algeo *et al.*[29] reported $\delta^{15}N$ and C/N ratio from the black shales of the Carboniferous period. They argued that the variation in denitrification ($\delta^{15}N$ of SOM) is because of eustatic changes during the glacial and interglacial periods. An increase (decrease) in denitrification is observed during the sea-level rise (fall) in interglacials (glacial). A similar pattern in denitrification was observed in Eastern Tropical Pacific Ocean over the past ~300 million years ago (Ma) (ref. 29). The $\delta^{15}N$ data from the anoxic ocean of lower Jurassic carbon-rich shales show a distinct positive $\delta^{15}N$ increase[30]. This was attributed to the upwelling of sub-oxic water mass similar to the Arabian Sea, Californian gulf, and the Peruvian coast. This development during the early Jurassic is also linked to increased organic productivity[30]. Only one record of sub-oxic conditions in the Arabian Sea since early Miocene (~25 Ma to present) exists from Maldives based on cores collected during the IODP Expedition 359 (ref. 31). They studied the redox-sensitive element Mn and found that from 25 to ~12.5 Ma, the sub-oxic conditions show a slightly increasing trend. At ~13 Ma, the sub-oxic condition suddenly strengthened showing the expansion of Arabian Sea OMZ to the core site and was stable till 5 Ma. Thereafter, the OMZ exhibits strong variability and finally retraction from the Maldives at around 0.8 Ma (ref. 31). The only record that reported denitrification ($\delta^{15}N$ of SOM) from the Arabian Sea since late Miocene (~10 Ma) suggests that the surface water productivity and OMZ remain weak from ~10 to ~3.2 Ma based on samples collected during the IODP Expedition 355 (Figure 2)[32]. Before that, the $\delta^{15}N$ record in the Arabian Sea extended till the last one million years (myr) only[33]. Figure 2, which is based on data from Tripathi *et al.*[32], shows the relation between denitrification variability and productivity from 10.2 Myr to present in Eastern Arabian Sea (Figure 2 *a–c*). The provenance of organic matter at the core site is determined from the $\delta^{13}C$ value of SOM and C/N ratio (Figure 2 *d* and *e*). These provenance proxies indicate that productivity is mostly of marine origin. Gaye-Haake *et al.*[34] showed that the $\delta^{15}N$ values of SOM vary from 6‰ to 11‰ in the Arabian Sea, which is based on surface sediment analysis of more than 100 locations in the Central and Eastern Arabian Sea. This is also noted by other studies[32,35]. Therefore, we consider a $\delta^{15}N$ value of 6‰ as an empirical threshold value indicating the presence of denitrification (shown by orange dashed line in Figure 2 *a*). The first time the $\delta^{15}N$ values are more than 6‰ is during the Mid-Pliocene Warm Period (MPWP; ~3 Ma). It suggests that the first appearance of denitrification occurred during MPWP and was supported by an increase in surface water productivity (Figure 2 *b* and *c*). MPWP is a period with similar conditions as today with similar atmospheric CO_2 concentration ~400 ppm (ref. 36), a mean annual temperature higher by 2.7°–4°C (ref. 37),

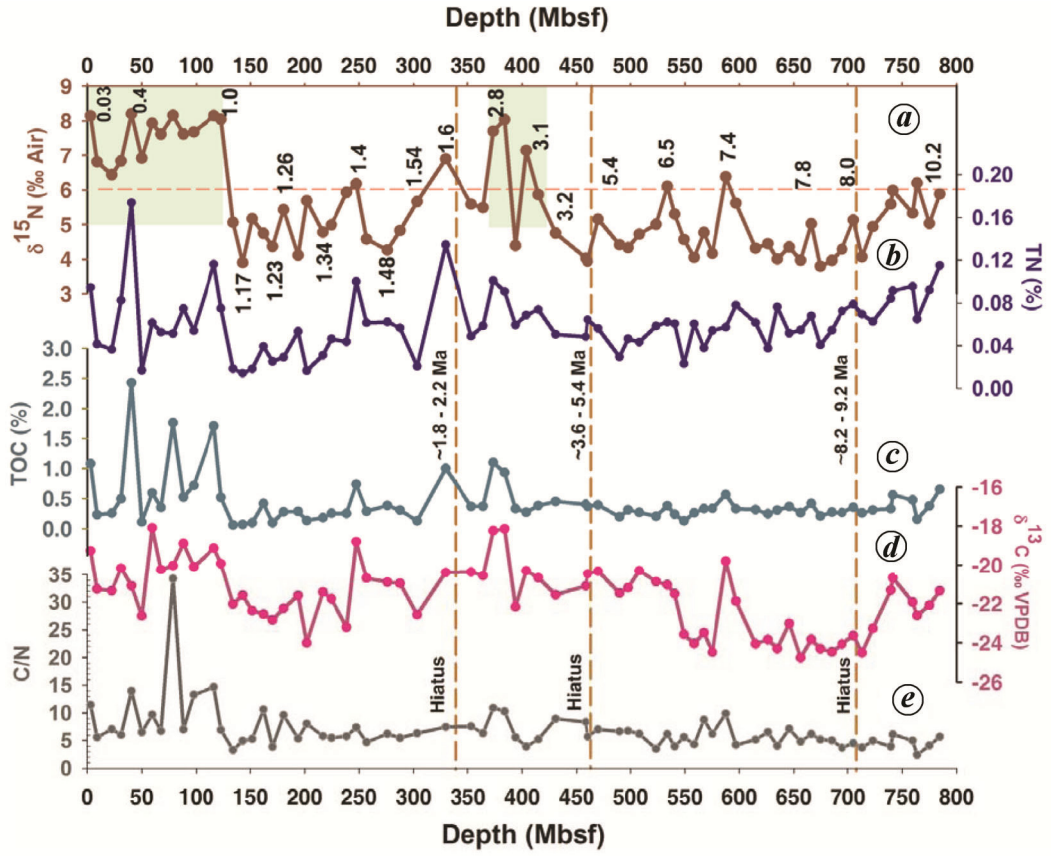

Figure 2. Denitrification record from the eastern Arabian Sea since the late Miocene. ***a***, Denitrification variability (δ^{15}N of SOM); ***b*** and ***c***, Past productivity variability (weight percent of total organic carbon and total nitrogen of SOM); ***d*** and ***e***, Provenance indicators (δ^{13}C and C/N ratio of SOM). The vertical broken lines indicate the position of the hiatuses. The horizontal dashed line over panel 'a' show denitrification threshold[32]. The age data (in million years ago, Ma) at site U1456 is shown by the Indo-Arabic numerals in panel 'a'. Redrawn after Tripathi *et al.*[32].

and the sea level higher by ~20 m than today[38]. The productivity increase during the MPWP could have further contributed to the intensification of the northern hemisphere glaciation by causing higher drawdown of CO_2. During 1.5 to 1 Ma, Tripathi *et al.*[32] found that the denitrification was either absent or very weak in the Arabian Sea. The denitrification again appeared at ~1 Ma as shown in Figure 2 *a*, reflecting the fact that the modern conditions in the Arabian Sea were attained by ~1 Ma.

Denitrification during MIS 15 to MIS 3 (~600 to 40 kyr) on multi-millennial timescale

The drilled section of U1457-A (17°N, 67°E; 3534 m water depth) was divided into four sections based on the sedimentology and analysed sediment samples from the Unit I (~120 m thick; Pleistocene nannofossil ooze interbedded with thin turbidites). This section spanned from ~600 kyr (MIS 15) to ~40 kyr (MIS 3). We further evaluated the SOM for digenetic alteration related to lithology. If there is any diagenesis, then there should be a correlation between TN and δ^{15}N. Earlier studies from the Western Arabian Sea[33] reported no correlation, which indicates that diagenesis does not affect δ^{15}N variation. We also obtain no relationship between δ^{15}N and TN ($r^2 = 0.19$; Supplementary Figure 1). Thus, diagenesis appears to cause no significant alteration in δ^{15}N values of SOM at Site U1457.

High-resolution δ^{15}N measurements from sediment samples of site U1457A show large variability; the δ^{15}N values range from around 3.4 to 9.1‰ with a mean value of 6.6‰. The marine denitrification causes an increase in δ^{15}N value which is significantly higher than the global ocean average nitrate value 4.5–6% as explained above[39]. Figure 3 shows the comparison of denitrification from both the eastern (Figure 3 *a*; present study; site U1457) and western Arabian Sea (Figure 3 *c*; ODP 722 B)[33] with productivity (Figure 3 *b*; present study; site U1457), and ventilation (Figure 3 *d*)[40]. Productivity is shown by the total nitrogen concentration at the core site (Figure 3 *b*). The ventilation variability is based on the δ^{13}C of the benthic foraminifera from the ODP site 722B from a water depth of ~2000 m (ref. 40). In the Arabian Sea, there is no record of ventilation of intermediate depths by AAIW (the depth in which denitrification takes place) for

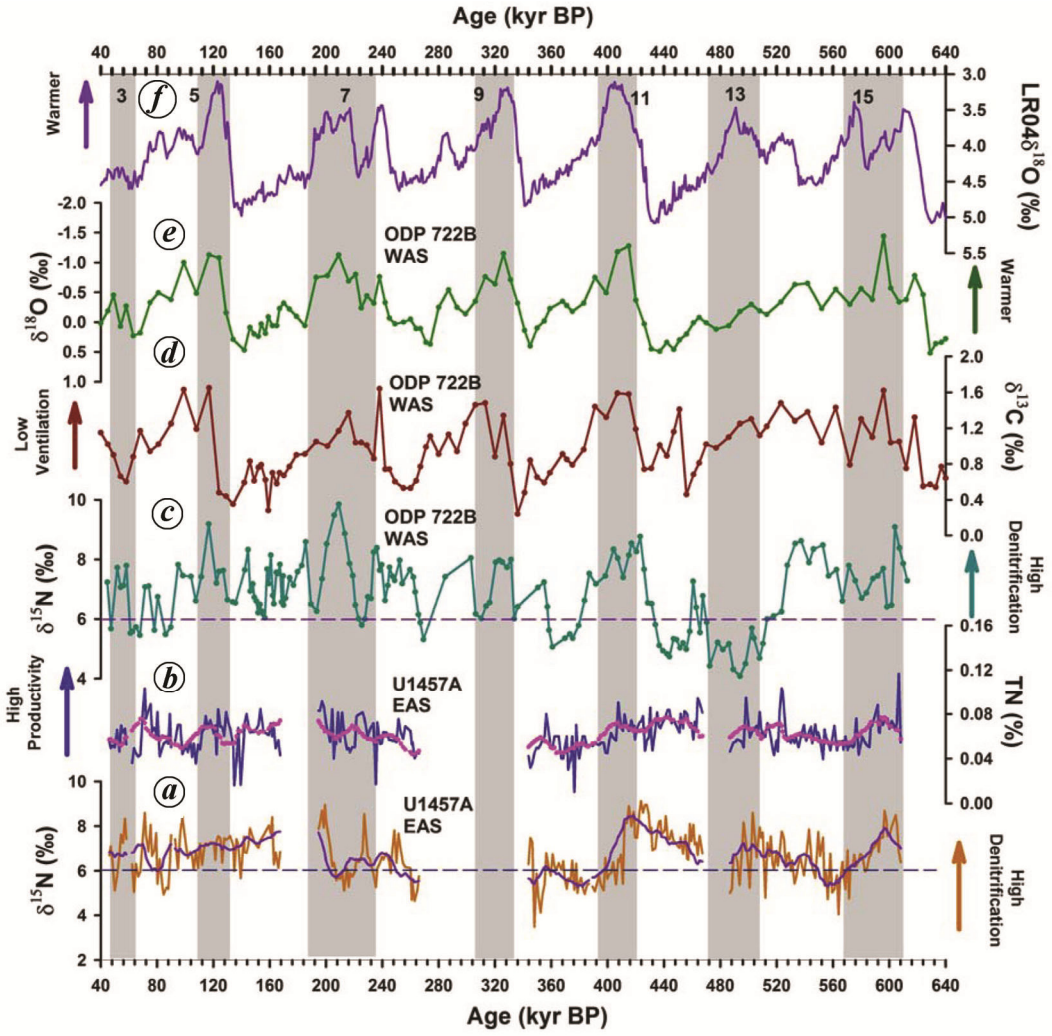

Figure 3. High-resolution denitrification variability from the eastern Arabian Sea (present study; site 1457A; panel (***a***) and its comparison with denitrification in the western Arabian Sea[33]; site 722B; panel (***c***). Panel (***b***) represents TN concentration of core 1457A related to productivity; (***d***) and (***e***) represent δ^{13}C and δ^{18}O variability from site 722B related to ventilation and global ice volume respectively[40]; panel (***f***) shows the LR04 stack (Lisiecki and Raymo, 2005) representing the glacial–interglacial cycles (the grey bands show the interglacial periods with corresponding MIS numbers).

the long period spanning the last 600 kyr. Therefore, we have chosen another record from the site 722B, which although belongs to a deeper depth, represents the strength of the influx of southern water masses into the Arabian Sea. So, it can indirectly indicate the AAIW variability. The δ^{13}C values of the benthic foraminifera have been used to reconstruct the past ventilation changes related to the age of the water[41]. The older water mass has more nutrient and low δ^{13}C value due to respiration, which releases the lighter isotope (^{12}C) into water. Presently, the North Indian Deep Water (NIDW) occupies the deeper parts of the Arabian Sea (~1500–3500 m). The NIDW is formed by the upwelling of the deep water from below 3500 m (ref. 42). The deep water is made up of high salinity cores of Antarctic Bottom Water (AABW), Circum Polar Deep Water (CDW), North Atlantic Deep Water (NADW) and Indian Deep Water (IDW)[43]. This deep water contains high nutrient and is aged water[43] and will, therefore, have lower δ^{13}C. As observed in Figure 3 *d*, higher (lower) δ^{13}C values during interglacial (glacial) show weakened (strengthened) ventilation by the southern water masses including AAIW. During MIS 15, the denitrification is strong but declines towards the glacial period (MIS 14) in both the eastern Arabian Sea (Figure 3 *a*) and western Arabian Sea (Figure 3 *c*). During interglacial periods like MIS 13, 11 and 9 (shown by grey bands, Figure 3), the denitrification is stronger in both the western and eastern Arabian Sea. The denitrification in the eastern Arabian Sea follows the productivity (Figure 3 *b*) and ventilation (Figure 3 *d*) variability within the chronological uncertainty. The increase in denitrification in both the western and eastern Arabian Sea during interglacials can be explained by the increase in productivity and a low influx of oxygen-rich intermediate water

(AAIW) to the core sites. The glacial periods (MIS 14, 12, 10 and 8) show low denitrification (lower δ^{15}N value) in both eastern (Figure 3 *a*) and western (Figure 3 *c*) Arabian Sea. The decrease in productivity during the glacial period results in the low denitrification. Further, the enhancement of oxygen-rich water during the colder period reduces the denitrification in both the eastern and western Arabian Sea. Earlier studies from the Arabian Sea and the Eastern Pacific, which reconstructed denitrification during late Quaternary, found stronger denitrification during interglacials and weaker denitrification during glacial periods[10,32,44] similar to the present study. From MIS 7 to MIS 3, the denitrification shows an overall decreasing trend, which is supported by enhanced ventilation by AAIW. The high-frequency variability shown by denitrification matches well with the productivity; denitrification was weak/strong during periods of low/high productivity.

Denitrification variability since the last glacial period (~70 kyr BP) on millennial timescale

Denitrification during Heinrich Events

Figure 4 shows the denitrification variability in the northern (Figure 4 *d*) and the western (Figure 4 *e* and *f*) Arabian Sea since the last glacial period along with the productivity (Figure 4 *h* and *g*) and ventilation (Figure 4 *c*) variability. The ventilation variability of the intermediate depth by the AAIW is based on the δ^{13}C of epibenthic foraminifera *Cibicidoides kullenbergi*[45]. Since the AAIW has higher δ^{13}C values than other water masses, high δ^{13}C reflects more ventilation by AAIW[45]. It is further compared with the GISP2 δ^{18}O record[46] showing past climate (temperature) variability. During colder periods (Heinrich events, H1 to H6 shown by grey bands), the decrease in sea level reduces the influx of marginal seawater (highly saline) to the Arabian Sea and it favours the northward circulation of southern water mass (low saline)[23,45]. Further, the low saline water coming from Indonesian throughflow (Banda Seawater) to the Arabian Sea[23,24] also acts as a barrier during the warmer period but its influx is lower during the colder period[27]. Thus, the meridional progression of oxygen-rich southern water mass to the Arabian Sea is enhanced during the colder period and it ventilates both the thermocline and intermediate depth in the Arabian Sea (shown by higher δ^{13}C values in Figure 4 *c*[45]. The ventilation of intermediate-depth reduces the OMZ as well as the denitrification during colder periods (lower δ^{15}N values in Figure 4 *d–f*). However, the southwest monsoon has an immense impact on denitrification and OMZ development. During colder period, the weakened southwest monsoonal upwelling results in lowered productivity in both western and northeastern Arabian Sea (Figure 4 *g* and *h*[44,47–49], which coincides with the decreased denitrification (grey bands in Figure 4)). It leads to the fact that the low organic matter influx due to lower productivity and the enhanced AAIW reduces the denitrification intensity during Heinrich events in western, northern and northeastern Arabian Sea. During LGM (~21 kyr), the decrease in SW monsoonal upwelling[50–52], reduced productivity coupled to enhanced ventilation by AAIW decreases denitrification intensity in the western region. In the northern Arabian Sea as well, the denitrification intensity is low. This may again be because of low organic matter advection from the western Arabian Sea coupled with higher ventilation. Although a few studies have suggested an increase in productivity during LGM[53,54] in the northern Arabian Sea due to an increase in winter monsoon-induced mixing, the reduced advection of organic matter along with higher ventilation reduces denitrification intensity[55,56].

Denitrification during last deglacial and Holocene period

The last deglaciation (18 kyr BP to 11 kyr BP) covers various colder (H1 and Younger Drays, YD) and warmer (Bølling–Allerød, B–A) periods that experienced varying inflow of AAIW into the Arabian Sea (Figure 4 *c*)[45,57]. The enhanced/reduced inflow of oxygen-rich water results in decreasing/increasing denitrification during colder/warmer periods of the deglaciation in both the northern and the western Arabian Sea (Figure 4 *d–f*). Further, the decrease (increase) in productivity (Figure 4 *g* and *h*) in the western Arabian Sea during the colder (warmer) periods adds to the decrease (increase) of the denitrification intensity[12,58].

The South Asian Summer Monsoon (SASM) was intensified in the early Holocene and declined from mid-Holocene (~5 kyr) to present[59–61]. The productivity trend in the western Arabian Sea follows southwest monsoon variability and the denitrification declines (Figure 4 *f*) during reduced monsoon-induced productivity as shown by Ba concentration (Figure 4 *h*)[47]. At the same time, the denitrification intensifies in north and northeastern Arabian sea during the Holocene period (Figure 4 *d*)[27]. This increase in denitrification is explained through intermediate water ventilation. The rise in sea level during the warmer period leads to increased inflow of oxygen-poor water from the Red Sea (RSW) and the Persian Gulf (PGW)[27]. The front created by this water acts as a barrier to the oxygen-rich southern water mass inflow to the northern Arabian Sea. Thus, the denitrification in the northern and northeastern Arabian Sea is heavily influenced by the ventilation of the intermediate water. But in the western Arabian Sea, the denitrification is mostly governed by the huge southwest monsoon-induced productivity variability leading to the divergent trends in

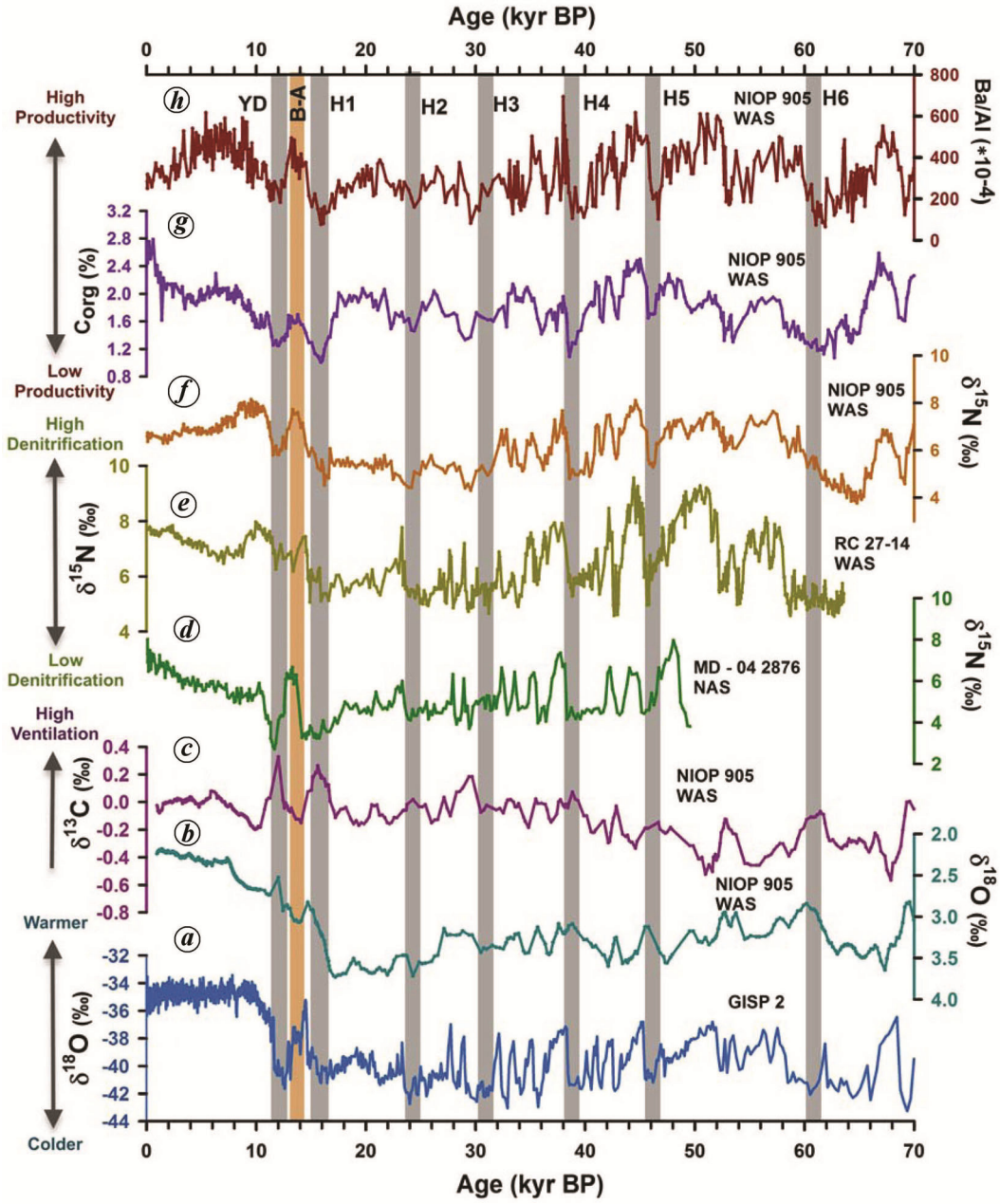

Figure 4. Comparison among denitrification variability from the western and eastern Arabian Sea, Northern Hemisphere temperature, and productivity from the western Arabian Sea. (***a***) The Greenland ice core δ^{18}O record GSIP 2 (ref. 46). (***b***) δ^{18}O and (***c***) δ^{13}C of benthic foraminifera (*C. kullenbergi*) of core NIOP 905 (ref. 45). (***d***) δ^{15}N of core MD-04 2876 from north Arabian Sea[27]. (***e***) δ^{15}N of core RC 27-14 from Oman margin[12]. (***f***) δ^{15}N, (***g***) organic carbon percentage and (***h***) Ba/Al ratio of core 905P (ref. 47). Grey bands represent colder periods (Henrich events, H1 to H6); dark orange bar indicates the Bølling-Allerød warm period; YD denotes Younger Dryas.

the denitrification in the western and northern Arabian Sea during Holocene.

Conclusion

The denitrification variability in the Arabian Sea is an interplay of monsoon-induced productivity and the ventilation by oxygen-rich southern water masses. The oldest record of δ^{15}N variability indicating denitrification intensity from the Arabian Sea spans the last 10 Myr. It shows that the denitrification first appeared at ~3 Ma, declined thereafter and attained modern strength by ~1 Ma. During the late Quaternary (last 600 kyr), the new data based on IODP Expedition 355 shows that the denitrification intensified during interglacials and weakened during the glacial periods. The comparison of denitrification variability from the eastern and western Arabian Sea since the last glacial period (past ~70 kyr) for which chronologically

well-constrained records are available shows similar variability, i.e. stronger (weaker) denitrification during warmer (colder) periods. During the Holocene, the sea level rise led to the influx of oxygen-poor RSW and PGW in the EAS. This reduced the inflow of oxygen-rich water from the Southern Ocean resulting in reduced ventilation of the northeastern Arabian Sea causing enhanced denitrification in contrast to the western Arabian Sea.

1. Paulmier, A. and Ruiz-Pino, D., Oxygen minimum zones (OMZs) in the modern ocean. *Prog. Oceanogr*., 2009, **80**, 113–128.
2. Qasim, S. Z., Oceanography of the northern Arabian Sea. *Deep Sea Res*., 1982, **29**, 1041–1068.
3. Naqvi, S. W. A., Some aspects of the oxygen deficient conditions and denitrification in the Arabian Sea. *Marine Res*., 1987, **29**, 459–469.
4. Olson, D. B., Hitchcock, G. L., Fine, R. A. and Warren, B. A., Maintenance of the low-oxygen layer in the central Arabian Sea. *Deep Sea Res. II*, 1993, **40**(3), 673–585.
5. Bange, H. W., Rapsomanikis, S. and Andreae, M. O., Nitrous oxide cycling in the Arabian Sea. *J. Geophys. Res*., 2001, **106**, 1053–1066.
6. Codispoti, L. A. and Richards, F. A., An analysis of the horizontal regime of denitrification in the eastern tropical North Pacific. *Limnol. Oceanogr*., 1976, **21**, 379–388.
7. Ward, B. B. *et al*., Denitrification as the dominant nitrogen loss process in the Arabian Sea. *Nature*, 2009, **461**, 78–81.
8. Cocco, V. *et al.*, Oxygen and indicators of stress for marine life in multi-model global warming projections. *Biogeosciences*, 2013, **10**, 1849–1868.
9. Keeling, R. F., Körtzinger, A. and Gruber, N., Ocean deoxygenation in a warming world. *Annu. Rev. Mar. Sci*., 2010, **2**(1), 199–229.
10. Altabet, M. A., Franqois, R., Murray, D. W. and Prell, W. L., Climate-related variations in denitrification in the Arabia Sea from 15N/14N ratios. *Nature*, 1995, **373**, 506–509.
11. Ganeshram, R. S., Pedersen, T. F., Calvert, S. E. and Murray, J. W., Large changes in oceanic nutrient inventories from glacial to interglacial periods. *Nature*, 1995, **376**, 755–758.
12. Altabet, M. A., Higginson, M. J. and Murray, D. W., The effect of millennial-scale changes in Arabian Sea denitrification on atmospheric CO_2. *Nature*, 2002, **415**(6868), 159.
13. Brandes, J. A. and Devol, A. H., A global marine-fixed nitrogen isotopic budget: implications for Holocene nitrogen cycling. *Global Biogeochem. Cycles*, 2002, **16**(4), 67–1.
14. Sigman, D. M., Altabet, M. A., McCorkle, D. C., Francois, R. and Fischer, G., The δ^{15}N of nitrate in the Southern Ocean: consumption of nitrate in surface waters. *Global Biogeochem. Cycles*, 1999, **13**(4), 1149–1166.
15. Naqvi, S. W. A., Narvekar, R. V. and Desa, E., Coastal biogeochemical processes in the North Indian Ocean. In *The Sea* (eds Robinson, A. and Brink, K.), Harvard University Press, 2006, vol. 14, pp. 723–780.
16. Brandes, J. A., Devol, A. H., Yoshinari, T., Jayakumar, D. A. and Naqvi, S. W. A., Isotopic composition of nitrate in the central Arabian Sea and eastern tropical North Pacific: a tracer for mixing and nitrogen cycles. *Limnol. Oceanogr*., 1998, **43**, 1680–1689.
17. Schäfer, P. and Ittekkot, V., Seasonal variability of δ^{15}N in settling particles in the Arabian Sea and its palaeogeochemical significance. *Naturwissenschaften*, 1993, **80**, 511–513.
18. Karl, D. *et al*., Dinitrogen fixation in the world's oceans. *Biogeochemistry*, 2002, **57/58**, 47–98.
19. Sigman, D. M., Karsh, K. L. and Casciotti, K. L., Ocean process tracers: nitrogen isotopes in the ocean. In *Encyclopedia of Ocean Sciences* (eds Steele, J. H., Turekian, K. K. and Thorpe, S. A.), Academic Press, London, 2009, 2nd edn, pp. 40–54.
20. Agnihotri, R., Bhattacharya, S. K., Sarin, M. M. and Somayajulu, B. L. K., Changes in surface productivity and subsurface denitrification during the Holocene: a multiproxy study from the eastern Arabian Sea. *The Holocene*, 2003, **13**(5), 701–713.
21. Wyrtki, K., Physical oceanography of the Indian Ocean. In *The Biology of the Indian Ocean*, Springer, Berlin, Heidelberg, 1973, pp. 18–36.
22. Swallow, J. C., Some aspects of the physical oceanography of the Indian Ocean. *Deep Sea Res Part A*, 1984, **31**(6–8), 639–650.
23. You, Y., Intermediate water circulation and ventilation of the Indian Ocean derived from water-mass contributions. *Marine Res*., 1998, **56**(5), 1029–1067.
24. Sharma, G. S., Gouveia, A. D. and Satyendranath, S., Incursion of Pacific Ocean water into Indian-Ocean. *Proc. Indian Acad. Sci. Section A*, 1978, **87**(3), 29–45.
25. Rohling, E. J. and Zachariasse, W. J., Red Sea outflow during the Last Glacial Maximum. *Quat. Int*., 1996, **31**, 77–83.
26. Fairbanks, R. C., A 17,000 year glacio-eustatic sea level record: influence of glacial melting rates on the Younger Dryas event and deep ocean circulation. *Nature*, 1989, **342**, 637–642.
27. Pichevin, L., Bard, E., Martinez, P. and Billy, I., Evidence of ventilation changes in the Arabian Sea during the late Quaternary: implication for denitrification and nitrous oxide emission. *Global Biogeochem. Cycles*, 2007, **21**(4), GB4008.
28. Pandey, D. K. *et al*., Site 1456. *Proc. Int. Ocean Discovery Prog*., 2016, **355**, 1–61.
29. Algeo, T., Rowe, H., Hower, J. C., Schwark, L., Herrmann, A. and Heckel, P., Changes in ocean denitrification during Late Carboniferous glacial–interglacial cycles. *Nat. Geosci*., 2008, **1**(10), 709.
30. Jenkyns, H. C., Gröcke, D. R. and Hesselbo, S. P., Nitrogen isotope evidence for water mass denitrification during the early Toarcian (Jurassic) oceanic anoxic event. *Paleoceanogr.*, 2001, **16**(6), 593–603.
31. Betzler, C., Eberli, G. P., Kroon, D., Wright, J. D., Swart, P. K., Nath, B. N. and Guo, J. A., The abrupt onset of the modern South Asian Monsoon winds. *Sci. Rep*., 2016, **6**, 29838.
32. Tripathi, S., Tiwari, M., Lee, J. and Khim, B. K., IODP Expedition 355 scientists, first evidence of denitrification vis-à-vis monsoon in the Arabian Sea since Late Miocene. *Sci. Rep*., 2017, **7**, 43056.
33. Altabet, M. A., Murray, D. W. and Prell, W. L., Climatically linked oscillations in Arabian Sea denitrification over the past 1 m.y.: implications for the marine N cycle. *Paleoceanogr.*, 1999, **14**, 732–743.
34. Gaye-Haake, B. *et al.*, Stable nitrogen isotopic ratios of sinking particles and sediments from the northern Indian Ocean. *Mar. Chem*., 2005, **96**(3–4), 243–255.
35. Gaye, B. *et al.*, Glacial–interglacial changes and Holocene variations in Arabian Sea denitrification. *Biogeosciences*, 2018, **15**(2), 507–527.
36. Pagani, M., Liu, Z., LaRiviere, J. and Ravelo, A. C., High Earth-system climate sensitivity determined from Pliocene carbon dioxide concentrations. *Nat. Geosci*., 2012, **3**(1), 27.
37. Haywood, A. M., Dowsett, H. J. and Dolan, A. M. Integrating geological archives and climate models for the mid-Pliocene warm period. *Nat. Commun*., 2016, **7**, 1–14; doi:10.1038/ncomms10646.
38. Miller, K. G. *et al.*, High tide of the warm Pliocene: implications of global sea level for Antarctic deglaciation. *Geology*, 2012, **40**(5), 407–410.
39. Sigman *et al*., Natural abundance-level measurement of the nitrogen isotopic composition of oceanic nitrate: an adaptation of the ammonia diffusion method. *Mar. Chem.*, 1997, **57**(3), 227–242.
40. Clemens, S. C., Murray, D. W. and Prell, W. L., Nonstationary phase of the Plio-Pleistocene Asian monsoon. *Science*, 1996, **274**(5289), 943–948.

41. Pierre, C., Vergnaud-Grazzini, C. and Faugeres, J. C., Oxygen and carbon stable isotope tracers of the water masses in the Central Brazil Basin. *Deep Sea Res. Part A*, 1991, **38**(5), 597–606.
42. Shetye, S. R., Gouveia, A. D. and Shenoi, S. S. C., Circulation and water masses of the Arabian Sea. *Proc. Indian Acad. Sci*., 1994, **103**, 107–123.
43. Tally, L. D., Pickard, G. L., Emery, W. J. and Swift, J. H., *Descriptive Physical Oceanography: An Introduction*, Elsevier, China, 2012, pp. 387–399.
44. Ganeshram, R. S., Pedersen, T. F., Calvert, S. E., McNeill, G. W. and Fontugne, M. R., Glacial-interglacial variability in denitrification in the world's oceans: causes and consequences, *Paleoceanogr.*, 2000, **15**(4), 361–376.
45. Jung, S. J., Kroon, D., Ganssen, G., Peeters, F. and Ganeshram, R., Enhanced Arabian Sea intermediate water flow during glacial North Atlantic cold phases. *Earth Planet Sci. Lett*., 2009, **280**(1–4), 220–228.
46. Grootes, P. M. and Stuiver, M., Oxygen 18/16 variability in Greenland snow and ice with 10–3- to 105-year time resolution. *J. Geophy. Res. – Oceans*, 1997, **102**(C12), 26455–26470.
47. Ivanochko, T. S., Ganeshram, R. S., Brummer, G. J. A., Ganssen, G., Jung, S. J., Moreton, S. G. and Kroon, D., Variations in tropical convection as an amplifier of global climate change at the millennial scale. *Earth Planet Sci. Lett*., 2005, **235**(1–2), 302–314.
48. Sirocko, F., Sarnthein, M., Erlenkeuser, H., Lange, H., Arnold, M. and Duplessy, J. C., Century-scale events in monsoonal climate over the past 24,000 years. *Nature*, 1993, **364**(6435), 322.
49. Singh, A. D., Jung, S. J., Darling, K., Ganeshram, R., Ivanochko, T. and Kroon, D., Productivity collapses in the Arabian Sea during glacial cold phases. *Paleoceanogr. Paleoclimtol.*, 2011, **26**(3).
50. Anderson, D. M. and Prell, W. L., A 300 kyr record of upwelling off Oman during the late Quaternary: evidence of the Asian southwest monsoon. *Paleoceanogr. Paleoclimatol*., 1993, **8**(2), 193–208.
51. Niitsuma, N., Oba, T. and Okada, M., Oxygen and carbon isotope stratigraphy at site 723, Oman margin. *Proc. Ocean Drilling Prog*., *Sci. Results*, 1991, **117**, 321–341.
52. Pattan, J. N., Masuzawa, T., Naidu, P. D., Parthiban, G. and Yamamoto, M., Productivity fluctuations in the southeastern Arabian Sea during the last 140 ka. *Palaeogeogr.*, *Palaeoclimatol*., *Palaeoecol*., 2003, **193**, 575–590.
53. Thamban, M., Rao, V. P., Schneider, R. R. and Grootes, P. M., Glacial to Holocene fluctuations in hydrography and productivity along the southwestern continental margin of India. *Palaeogeogr.*, *Palaeoclimatol.*, *Palaeoecol*., 2001, **165**(1–2), 113–127.
54. Cabarcos, E., Flores, J. A., Singh, A. D. and Sierro, F. J., Monsoonal dynamics and evolution of the primary productivity in the eastern Arabian Sea over the past 30 ka. *Palaeogeogr.*, *Palaeoclimatol.*, *Palaeoecol*., 2014, **411**, 249–256.
55. Rostek, F., Bard, E., Beaufort, L., Sonzogni, C. and Ganssen, G., Sea surface temperature and productivity records for the past 240 kyr in the Arabian Sea. *Deep Sea Res. II*, 1997, **44**, 1461–1480.
56. Schulte, S., Rostek, F., Bard, E., Rullkötter, J. and Marchal, O., Variations of oxygen-minimum and primary productivity recorded in sediments of the Arabian Sea. *Earth Planet Sci. Lett*., 1999, **173**(3), 205–221.
57. Yu, Z. *et al.*, Antarctic Intermediate water penetration into the Northern Indian Ocean during the last deglaciation. *Earth Planet Sci. Lett*., 2018, **500**, 67–75.
58. Suthhof, A., Ittekkot, V. and Gaye-Haake, B., Millennial-scale oscillation of denitrification intensity in the Arabian Sea during the Late Quaternary and its potential influence on atmospheric N_2O and global climate. *Global Biogeochem. Cycles*, 2001, **15**(3), 637–649.
59. Hong, Y. T., Hong, B., Lin, Q. H., Zhu, Y. X., Shibata, Y., Hirota, M. and Wang, H., Correlation between Indian Ocean summer monsoon and North Atlantic climate during the Holocene. *Earth Planet Sci. Lett*., 2003, **211**(3–4), 371–380.
60. Tiwari, M., Nagoji, S. S. and Ganeshram, R. S., Multi-centennial scale SST and Indian summer monsoon precipitation variability since the mid-Holocene and its nonlinear response to solar activity. *Holocene*, 2015, **25**(9), 1415–1424.
61. Nagoji, S. S. and Tiwari, M., Organic carbon preservation in Southeastern Arabian Sea sediments since mid-Holocene: implications to South Asian Summer Monsoon variability. *Geochem. Geophys*., 2017, **18**(9), 3438–3451.

ACKNOWLEDGEMENTS. We are grateful to the Secretary, Ministry of Earth Sciences and Director, NCPOR for support and encouragement (NCAOR Contribution No. J-19/2020–21). We thank the IODP and the colleagues and the crew onboard IODP Expedition 355 for making this study possible. This research has also been supported by the Research Council of Norway (RCN) and MoES, Government of India through the Ind-Nor programme (grant no. 248793 and MoES/Ind-Nor/PS-8/2015).

doi: 10.18520/cs/v119/i2/282-290